[see (3.19)] are *not* the same as the average bulk interaction $J_\Gamma(\vec{R}_{||})$.

[15]The optimized inequality (4.23) is approximately correct when ν^* determined by (4.22) is near an integer. It is not a good approximation at high temperatures when the solution of (4.22) becomes $\nu^* < 1$. This indicates that $\nu = 1$ (no corridor) is then optimal. See Sec. V for numerical examples.

[16]Strictly speaking, we have again established this result only for the cases in which the monotonic decreasing bound $J_0(|\vec{R}_{||}|)$ exists, since it is not immediately obvious that the nonintegrability of $[\hat{J}_\Gamma(\vec{0}) - \hat{J}_\Gamma(\vec{k}_{||})]^{-1}$ implies that $\mu_1(\Gamma)/\mathfrak{N}(\Gamma) \to 0$ as $\mathfrak{N}(\Gamma) \to \infty$. It is not worthwhile, however, to worry about possible pathological cases in this connection.

[17]T. Matsubara and H. Matsuda, Progr. Theoret. Phys. (Kyoto) 16, 569 (1956); R. Whitlock and P. Zilsel, Phys. Rev. 131, 2409 (1963); M. E. Fisher, Rept. Progr. Phys. 30, 615 (1967).

[18]As stated previously, the absence of long-range order is established even when transverse fields are present in the corridor Δ. However, to simplify the numerical analysis they are assumed to vanish.

[19]J. Ginibre in Lectures given at the Cargèse Summer School in Statistical Mechanics, 1969 (unpublished); C. A. Hurst and S. Sherman, Phys. Rev. Letters 22, 1357 (1969); G. Gallavotti (unpublished).

[20]The bounds obtained have been for subdomains Γ which were "slices" as shown in Fig. 1. We may obtain bounds for a general subdomain Θ in the case $f(\vec{r}) \equiv 1$ once the non-negativity of $\sigma(\vec{r}, \vec{r}')$ has been established. It then follows that $\Psi_\Omega\{1 \mid \Theta\} \leq \Psi_\Omega\{1 \mid \Gamma\}$ provided $\Theta \subset \Gamma$.

[21]Notice that $\bar{\sigma}_\infty(\vec{r}, \vec{r}') = \sigma_\infty(\vec{r}, \vec{r}')$ when $\mathfrak{N}_y = \mathfrak{N}_z = 1$ $(d=1)$ and when $\mathfrak{N}_z = 1$ $(d=2)$.

PHYSICAL REVIEW B VOLUME 3, NUMBER 3 1 FEBRUARY 1971

Specific Heat of Nickel near the Curie Temperature*

D. L. Connelly, J. S. Loomis, and D. E. Mapother
Department of Physics and Materials Research Laboratory, University of Illinois, Urbana, Illinois 61801
(Received 6 August 1970)

Using an ac calorimetric method, the specific heat $C_p(T)$ of pure single-crystalline Ni has been measured over a temperature range of 100 K centered at the Curie point (~ 631 K). The experimental method permits continuous observation of C_p vs T with a temperature resolution of ~0.01 K using very small specimens (~7.8 mg). Special attention has been devoted to the determination of the analytical form of the magnetic contribution to $C_p(T)$. The effect of applied fields up to 240 Oe has also been studied. At zero field, the data fit a standard power-law expression over the range $-3.2 \leq \log_{10}|(T-T_c)/T_c| \leq -1.6$, with exponents $\alpha = \alpha' = -0.10 \pm 0.03$. The data obtained with applied field follow the scaling relations calculated by Griffiths from the magnetic equation of state. The observed rounding of the specific-heat curve at its maximum is discussed and some experimental factors which influence the degree of the observed rounding are described.

I. INTRODUCTION

This paper reports an experimental study of the temperature dependence of the specific heat $C_P(T)$ for Ni near its Curie point ($T_C \simeq 631$ K). The measurements are made using an ac calorimetric technique which permits direct observation of $C_p(T)$ as a continuous function of T (with a temperature resolution of about 10^{-2} K) on small specimens of mass about 10 mg. These experimental advantages permit unusually precise examination of $C_p(T)$ near the singularity at T_C using very small specimens of relatively high crystalline perfection.

The ac calorimetric method used here is an elaboration of a basic technique originally developed and described independently by Kraftmakher[1] and by Sullivan and Seidel.[2] A previous account outlining the essential details of the present method and giving some preliminary data for Ni was published earlier.[3] The results reported here are believed to give a more detailed picture of the form of the singularity in $C_p(T)$ for Ni than any of the previously reported investigations. Preliminary results on the effect of an applied magnetic field and some of the physical factors which affect the shape of the singularity are also described.

II. EXPERIMENTAL METHOD

A. Technique

The same technical principles described earlier[3] are used here, but several refinements have been made. The principal changes are intended to (a) increase the sensitivity and precision of the temperature measurements and (b) improve the quality of the measured Ni specimens.

The Ni specimens are single-crystal chips (3 $\times 3 \times 0.1$ mm) lightly supported in the center of a massive copper assembly which occupies the center of a furnace. The dominant thermal contact between the specimen and the copper surroundings is

provided by He exchange gas ($p \simeq 350$ mm of Hg). The furnace is equipped with an automatic regulating and programming control which permits the ambient temperature to be swept past the transition temperature T_C at a predetermined rate. Specimen temperature is monitored by a thermocouple junction created by spot welding chromel and constantan thermocouple wire to the back face of the sample. The wires, originally 0.0007 in. diam, were flattened before welding to form ribbons 70×5 μ thick.

Light from a tungsten filament bulb[4] is passed through a rotary chopper to give square-wave heating pulses and is focused on the blackened front face of the specimen. The average light intensity falling on the specimen causes its temperature to rise, typically 0.5 K above that of the surroundings, as measured by the sample thermocouple. Superimposed on this dc temperature difference is a triangular pattern of temperature oscillations with a typical peak-to-peak magnitude of about 0.016 K. A phase-sensitive lock-in amplifier (Princeton Applied Research Model No. HR8) measured the rms magnitude of the fundamental harmonic of these sample temperature oscillations, referred to the phase of the incoming light.

As shown in more detail by Sullivan and Seidel,[2] two time constants serve to characterize the thermal dynamics of the system. One time constant, τ_1, characterizes the thermal coupling between the sample and its surroundings, which in the present case is provided by the He exchange gas. The other time constant, τ_2, characterizes the thermal relaxation within the sample and is determined by the diffusivity and thickness of the sample. The use of chopped light for heating and the negligibly small thermocouple junction spot welded directly to the sample as a thermometer eliminate the need for corrections due to the specific heat and thermal lag of the heater and thermometer. Under the conditions that $\omega\tau_1 \gg 1$ and $\omega\tau_2 \ll 1$ (where ω is the angular frequency of the light pulses), Sullivan and Seidel obtain for the magnitude of the ac temperature oscillations θ

$$\theta = \dot{Q}(\omega C_p)^{-1}[1 + (\omega\tau_1)^{-2} + \tfrac{1}{90}(\omega\tau_2)^2 + \tfrac{2}{3}(\tau_2/\tau_1)]^{-1/2},$$

where C_p is the heat capacity of the sample and $\dot{Q}$ is the maximum rate of radiant-energy absorption.

The present experimental arrangement differs from the case analyzed by Sullivan and Seidel in the following respect: Although heat is added to only the front face of the specimen slab, heat loss occurs via exchange-gas coupling from *both* the front and back faces of the slab. However, this fact requires modification of the equation for θ only for measuring frequencies where the period becomes comparable with the relaxation time for the propagation of heat through the thickness of the slab (about 0.001 sec for the Ni specimens used). At the measuring frequencies used here (< 60 Hz) no significant error results from lumping the heat transfer from both front and back faces of the slab into a single conductance factor with the associated time constant τ_1.

The time constants, τ_1 and τ_2, both involve the heat capacity of the specimen and hence are temperature dependent. However, the term $\frac{2}{3}(\tau_1/\tau_2)$ is estimated to about 0.1% of the bracketed expression and independent of the specimen heat capacity. The contributions of the terms involving $\omega\tau_1$ and $\omega\tau_2$ show negligible variation within a suitably chosen range of ω. This may be demonstrated experimentally by observing the variation in the product, $\omega\theta$, as a function of frequency. Such measurements showed the variation of $\omega\theta$ to be less than 1% within the range from 25 Hz to over 60 Hz with the present apparatus.

Since θ is directly proportional to $\dot{Q}$, it is essentil that the light intensity be precisely controlled. Satisfactory stability was achieved by powering the light bulb from a Sorenson Q Nobatron QRC20-8 dc power supply operated in the voltage-stabilizing mode. The lamp current was continuously monitored by measuring the voltage across a precision resistor in series with the lamp and was usually constant to 0.03% over a run lasting several hours. Light intensity was independently monitored by using a small quartz "light pipe" to deflect a fraction of the modulated incident light beam to a sensitive radiation thermocouple.[5] Periodic observations indicated the light intensity remained constant to at least 0.4% over a run lasting several hours and the data can be corrected for any observed fluctuations.

The temperature of the furnace is measured by a four-junction chromel constantan thermopile which was occasionally calibrated using a Pt resistance thermometer mounted in place of a sample. The absolute precision of the temperature measurement was about ± 0.2 K. The relative sensitivity of the measurement of sample temperature was limited by the size of the ac oscillations in the sample (0.016 K peak to peak).

The emf generated by the thermopile is balanced by a precise dc potentiometer which provides a constant emf corresponding to a furnace temperature near T_C. The difference emf is then amplified by a Hewlett-Packard 425A voltmeter and sent to the x axis of an x-y recorder. The maximum sensitivity range used gave 0.125 K per inch of chart paper, with a resolution of about ± 8 mK. A measurement of the sample thermocouple was made separately by a Leeds and Northrup K5 potentiometer at intervals during a run. The actual sample temperature is obtained by adding this to the furnace temperature.

The output from the HR8 (inverse specific heat) is presented to the y axis of the recorder. The final sensitivity is equivalent to a resolution of about ± 0.05 J/mole K. Some improvement in the signal-to-noise ratio was obtained by driving the synchronous motor of the light chopper from a stabilized frequency source.[6]

Furnace temperature was cycled over a predetermined range $T_C \pm 12$ K in a typical run. Experiments at different (but constant) rates of temperature change showed the shape of the specific-heat curve to be independent of sweep rate for speeds from 60 mK/min to approximately 0.4 K/min.

A typical run is presented in Fig. 1 and shows the detail obtained near the peak. This particular curve was traced at a rate of 60 mK/min. The output of the HR8 and the thermopile emf were also recorded continuously against time on a multichannel chart recorder. This gave a permanent record of the time variation of the furnace temperature and separate indications of the noise level of the thermopile and sample thermocouple signals.

B. Sample Preparation

Single-crystal nickel samples were prepared from a crystal grown from 99.999% starting material.[7] Slices about 0.015 in. thick were cut by spark erosion from this crystal and mechanically polished with No. 600 SiC paper and 6-μm diamond polish to a uniform thickness of about 0.009 in. The slices were then electropolished to 0.005 in. using a solution of "Electro-glo 300"[8] with a 4-V potential for 5–7 min. They were then waxed onto glass plates and diced into square chips using a string saw. After dicing, the samples were cleaned in acetone and annealed in vacuum at 750 °C for 4–6 h.

Mass-spectrographic analysis of one single-crystal nickel chip as prepared for measurement showed 800 ppm Co, 100 ppm Fe, and 60 ppm Cu to be the principle impurities. Analysis of a sample of the starting material for the single crystal indicated less than 5 ppm for these impurities. Polycrystalline material from the same source[7] in the form of 0.001-in.-thick foil showed 3.5 ppm Co, 8 ppm Fe, and 1.5 ppm Cu to be the principal metallic impurities. Samples were cut from this sheet, cleaned in acetone, and annealed as described above.

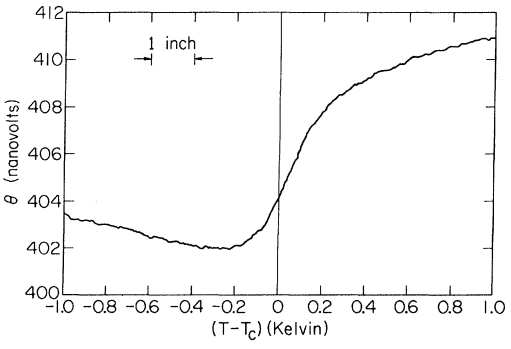

FIG. 1. Typical X-Y-recorder tracing showing the variation of lock-in amplifier signal with temperature near the Curie point of Ni. This section of the curve was traced at a sweep rate of about 1 mK/sec.

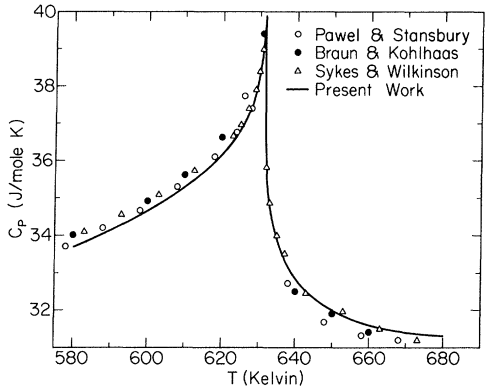

FIG. 2. Comparison of experimental C_p data for Ni. Values from Refs. 9–11 are shown by discrete points while the smooth curve is drawn through the data of Table I.

III. RESULTS AND ANALYSIS

A. Specific-Heat Data in Zero Field

Data obtained with the applied field $H = 0$ are collected in Table I and plotted in Fig. 2. Our ac calorimetric method gives only relative values of C_p. Absolute values of C_p are assigned by normalizing to fit the average of published absolute measurements[9–11] over a range of 100 K centered at T_C. Further analysis is required to separate the contribution to C_p associated with the magnetic transition at the Curie point.

1. *Magnetic Contribution to C_p*

The calculation of the magnetic contribution to C_p has been discussed recently for the case of Ni by Pawel and Stansbury.[12] We have followed their analysis to express our measured C_p values as C_v^*, the magnetic contribution to the specific heat at constant volume, where

$$C_v^* = C_p - Tv\beta^2/K_T - C_{v(\text{lattice})} - C_e \, .$$

In this equation C_p is the normalized experimental value, $C_{p(\text{lattice})}$ and C_e are the same expressions given by Pawel and Stansbury, and V, β, and K_T are the molar volume, volume expansivity, and isothermal compressibility, respectively.

Evaluation of the term $Tv\beta^2/K_T$ is complicated by the fact that both β and K_T change slightly near T_C. We have used the approximate relations

$$C_p = v\lambda T_C \beta + C_1 ,$$

$$K_T = \beta/\lambda + C_2 ,$$

where $\lambda \equiv (dP/dT)_{T=T_C}$ (i.e., the slope of the transition line in the P-T plane), and C_1 and C_2 are constants. These equations have been proposed by Pippard[13] and are expected to be valid near a critical point. Direct measurements on Ni by Patrick[14] yield the value $\lambda = (2.86 \pm 0.17) \times 10^3$ atm/K, from which we obtain $v\lambda T_C = 1.17 \times 10^6$ J/mole. Considering experimental error, this is in reasonable agreement with the value of 0.7×10^6 J/mole obtained by plotting C_p vs β from the expansivity measurements of Nix and MacNair.[15] This plot also indicates the constant C_1 to be negligible. The term β/λ in the expression for K_T gives only a 3% contribution and is ignored. Thus we obtain the approximation

$$Tv\beta^2/K_T \approx (C_p/\lambda)^2 (vTK_T)^{-1}$$

and the magnitude of this term is shown for comparison with the calculated C_v^* in Fig. 3.

TABLE I. Specific heat of single-crystal nickel at constant pressure and estimated contribution to the magnetic specific heat at constant volume.

T (K)	C_p (J/mole K)	C_v^* (J/mole K)	T (K)	C_p (J/mole K)	C_v^* (J/mole K)
580.00	33.70	4.39	631.60	38.70	8.28
582.00	33.79	4.45	631.65	37.73	7.44
584.00	33.85	4.48	631.70	37.11	6.90
586.00	33.95	4.56	631.75	36.69	6.53
588.00	34.03	4.60	631.80	36.40	6.27
590.00	34.13	4.66	631.85	36.22	6.12
592.00	34.21	4.72	631.90	36.06	5.97
594.00	34.32	4.80	631.95	35.90	5.83
596.00	34.42	4.87	632.00	35.81	5.75
598.00	34.54	4.96	632.10	35.61	5.58
600.00	34.65	5.04	632.20	35.45	5.44
602.00	34.77	5.13	632.30	35.31	5.31
604.00	34.91	5.23	632.40	35.20	5.21
606.00	35.03	5.32	632.50	35.09	5.12
608.00	35.15	5.40	633.00	34.68	4.75
610.00	35.28	5.50	633.50	34.37	4.47
612.00	35.42	5.60	634.00	34.13	4.26
614.00	35.58	4.73	634.50	33.97	4.11
616.00	35.77	5.87	635.00	33.80	3.95
618.00	35.95	6.01	635.50	33.66	3.83
620.00	36.16	6.18	636.00	33.53	3.71
621.00	36.27	6.26	636.50	33.41	3.60
622.00	36.39	6.36	637.00	33.31	3.50
623.00	36.52	6.46	637.50	33.20	3.40
624.00	36.66	6.58	638.00	33.11	3.32
625.00	36.83	6.72	638.50	33.02	3.23
625.50	36.91	6.78	639.00	32.94	3.16
626.00	37.00	6.86	639.50	32.87	3.09
626.50	37.10	6.94	640.00	32.80	3.02
627.00	37.20	7.02	640.50	32.73	2.96
627.50	37.32	7.12	641.00	32.67	2.90
628.00	37.44	7.22	642.00	32.57	2.80
628.50	37.57	7.33	643.00	32.50	2.73
629.00	37.76	7.49	644.00	32.42	2.65
629.50	37.99	7.69	646.00	32.25	2.48
630.00	38.26	7.92	648.00	32.13	2.36
630.50	38.59	8.20	650.00	32.01	2.23
630.60	38.68	8.28	652.00	31.91	2.13
630.70	38.75	8.33	654.00	31.83	2.04
630.80	38.85	8.42	656.00	31.74	1.94
630.90	38.97	8.52	658.00	31.67	1.86
631.00	39.10	8.64	660.00	31.61	1.79
631.05	39.18	8.70	662.00	31.55	1.72
631.10	39.26	8.77	664.00	31.50	1.66
631.15	39.35	8.85	666.00	31.47	1.62
631.20	39.45	8.94	668.00	31.43	1.56
631.25	39.55	9.02	670.00	31.40	1.52
631.30	39.65	9.11	672.00	31.38	1.49
631.35	39.76	9.20	674.00	31.35	1.44
631.40	39.86	9.29	676.00	31.33	1.41
631.45	39.90	9.32	678.00	31.31	1.37
631.50	39.83	9.26	680.00	31.30	1.35
631.55	39.43	8.92			

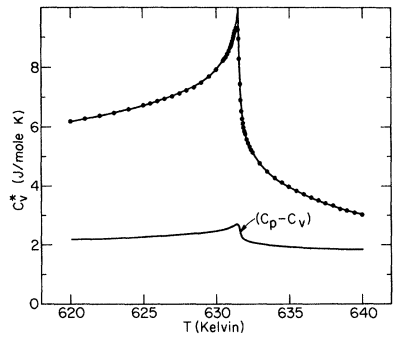

FIG. 3. Magnetic specific heat C_v^* near the Curie point of Ni. Continuous curve through the points gives the analytic fit to (1) described in the text. Lower curve gives the correction term Tv^2/K_T subtracted from C_p to obtain C_v.

It should be remarked that the calculated transformation from C_p to C_v^* has very slight effect on the subsequent analysis of the temperature dependence of the heat capacity. If the analysis (to be described in Sec. III A 2) to determine the power-law exponents α and α' is performed on the uncorrected experimental $C_p(T)$ data, the values of the exponents obtained differ by about 0.03 from the values obtained using $C_v^*(T)$, which is about the size of the experimental uncertainty in the determination of the α's.

2. *Power-Law Fitting*

The experimentally derived values of C_v^* have been fitted to the expression

$$C(t) \equiv (A/\alpha) t^{-\alpha} + K , \qquad (1)$$

where $t = |T - T_C|/T_C$.[16] The constants α, A, and K are used to represent the temperature range above T_C while primed constants in the same equation describe the temperature range below T_C. As shown by the solid curves of Figs. 3 and 4, use of

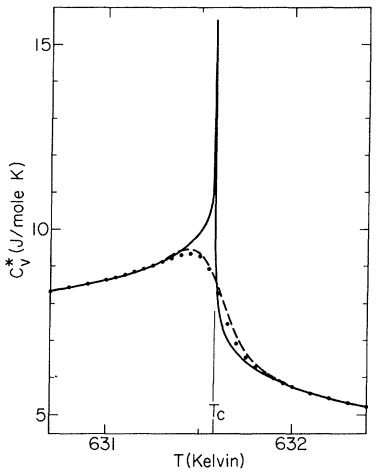

FIG. 4. Temperature variation of the magnetic specific heat very close to the Curie point. Data points are from Table I. Solid curve shows the analytic fit to (1) with $T_c = 631.58$ K and $\alpha = \alpha' = -0.10$. The dashed curve is calculated using the Gaussian distribution function described in the text.

(1) provides a satisfactory fit of the experimental data except for a temperature interval of about 0.25 K above and below the maximum in C_v^*. Within this interval the specific heat shows a "rounded" peak instead of the sharp rise expected from (1) at small values of t.

This rounded appearance of the maximum in C_v^* (T) is one of the most consistently reproducible features of the measurement, being observed essentially unchanged on six different single-crystal specimens. We conclude that the rounding must be treated as a real effect in the transitions of these specimens and, accordingly, experimental data lying within the rounded region are excluded from the analysis used to deduce the constants in (1).

The use of (1) to determine the exponents α and α' is complicated by uncertainty regarding the proper choice of T_C. Unfortunately, the criteria for defining T_C from rounded experimental data are somewhat subjective and imprecise. In previous work, it has been considered self-evident that T_C should correspond to the value at which the maximum value occurs in C_v. The present results suggest that this criterion may be incorrect.

Taking advantage of the high resolution and smoothness of the present data, we have analyzed our experimental data using

$$\log_{10}\left|\frac{dC}{dT}\right| = -(\alpha+1)\log_{10}t + \log_{10}A, \qquad (2)$$

which is obtained by differentiation of (1). In addition to displaying α explicitly, (2) shows the range of t for which (1) is valid by the linearity of the curve which results when experimental values of $|dC/dT|$ vs t are plotted logarithmically. Of course, to make such a plot it is necessary to choose a value for T_C, and it is important to appreciate the effect of error in the chosen value. This is illustrated for a hypothetical case in Fig. 5.

The behavior of (2) for a mathematically exact power law is plotted as the solid line in Fig. 5. The dashed curves show the effect of changing T_C by the indicated small amounts. For $\log_{10}t < -3$, curvature is easily recognized, but for $\log_{10} > -3$, the curvature is so slight that the effect of changing T_C is indistinguishable in practice from a shift in the value of α. Experimental data plotted according to (2) are presented in Fig. 6 for $T_C = 631.58$ K and show satisfactory linearity over almost two decades of t above and below T_C. However, it is not possible to choose a value of T_C which will eliminate the

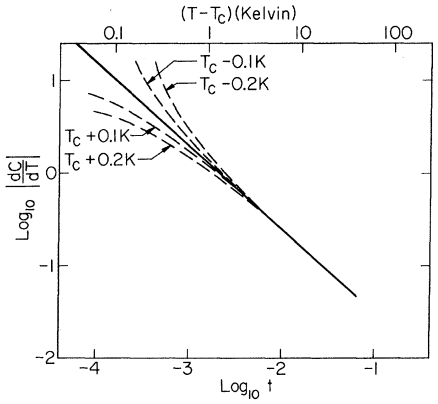

FIG. 5. Effect of uncertainty in T_C on the apparent linearity of (2). Dashed curves show the effect of shifting the value of T_C by the indicated amounts.

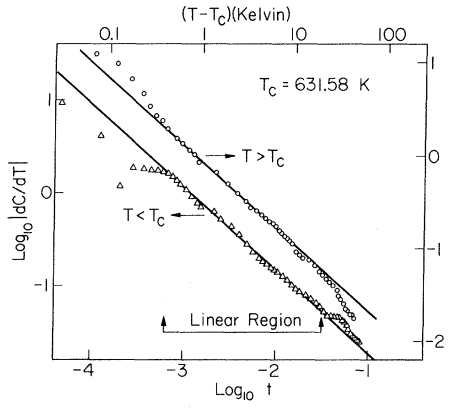

FIG. 6. Data of Table I plotted according to (2). Straight lines indicate the exact power law with $\alpha = \alpha' = 0.10$. The origin on the ordinate has been displaced to distinguish data measured above and below T_C.

rounding that becomes apparent for $\log_{10} t < -3.2$, and, as already remarked, data points within this range are excluded from the power-law analysis. As shown in Fig. 5, reasonable linearity may be obtained for the remaining data (at larger values of $\log_{10} t$) for choices of T_C over a range of several tenths of a degree. In short, the linearity of (2) in itself is insufficient as a criterion for fixing either T_C or the α's precisely.

Our approach to this ambiguous situation is to treat T_C as an adjustable parameter and study the variation of α and α' over a range of T_C values near the maximum in C_v^*. This variation is shown in Fig. 7 where it is seen that the α and α' curves cross for a choice of $T_C \sim 0.13$ K above the maximum of the C_v^* curve. Statistical uncertainty in the α values derived by least-squares analysis of (2) is indicated by the parameter σ.

It is evident from Fig. 7 that a variation of 0.1 K in the choice of T_C leads to substantial change in the α values. If T_C is chosen to correspond to the maximum in C_v^*, the resulting values of the exponents are $\alpha = 0.00$ and $\alpha' = -0.18$ in agreement with other recently reported measurements on Ni.[3,17] However, the fact that the exponents differ is inconsistent with theoretical arguments[18] which require that $\alpha = \alpha'$.

Considering the subjective elements which enter into the analysis of such data, it seems that choosing T_C at the crossover point has more fundamental justification than choosing it at the maximum of C_v^*. Furthermore, statistical analysis shows the rms deviation of the experimental data from (1) to vary slightly with the chosen value of T_C, and it passes through a weak minimum near the crossover point. The variation in the quality of the fit is not sufficiently pronounced to be decisive in itself, but, considering the theoretical arguments for equal exponents, we believe that choosing T_C at the crossover point provides the best interpretation of these data. Applying this criterion, we obtain $T_C = 631.58$ K from which value it follows by least-squares analysis that

$$\text{for } T > T_C, \quad \alpha = -0.10 \pm 0.03 ,$$
$$A = 1.609 \pm 0.005 \text{ J/mole K} ,$$
$$K = 13.49 \pm 0.03 \text{ J/mole K} ;$$
$$\text{for } T < T_C, \quad \alpha' = -0.10 \pm 0.03 ,$$
$$A' = 1.416 \pm 0.005 \text{ J/mole K} ,$$
$$K' = 15.67 \pm 0.03 \text{ J/mole K} .$$

These are the constants used to calculate the solid curves shown in Figs. 3 and 4. From these figures it is evident that the upper and lower branches of (1) give a satisfactory representation of the experimental data except for the region of about 0.5 K near T_C. Within this region, the distinctive features of (1) are (a) the extremely sharp rise of the analytic expression as $t \to 0$, and (b) a discontinuity $\Delta = K' - K = 2.18$ J/mole K at T_C.

As already remarked, the experimental data fail to follow the power-law increase for $t < 3 \times 10^{-4}$, but there is clear evidence of the discontinuity in the general downward shift of C_v^* values for $T > T_C$. This suggests that the transition region in the actual Ni specimens follows a smeared out discontinuity instead of the sharp step expected on the basis of (1). Two approaches to an analytical description of the experimentally observed transition region are described in Sec. III A 3.

3. *Analytic Representation of C_v^* near T_C*

Near T_C, the experimental data can be represented by an interpolation function $h(T)$ introduced to describe the rounded discontinuity exhibited by the measured points. To construct $h(T)$ we define the continuous power-law function

$$F(T) \equiv (A/\alpha) t^{-\alpha} + K \quad \text{for } T > T_C , \tag{3a}$$
$$F(T) \equiv (A'/\alpha') t^{-\alpha'} + K \quad \text{for } T < T_C . \tag{3b}$$

Note that K is used instead of K' in (3b) so that $F(T)$ is continuous, showing a cusp at T_C instead of the discontinuity ($\Delta = K' - K$) shown by (1). The desired interpolation function is now defined as

$$h(T) \equiv C_v^*(T) - F(T) , \tag{4}$$

where $C_v^*(T)$ represents the observed data points.

If $F(T)$ is evaluated using the constants α, α', A, A', and K (obtained in Sec. III A 2), substitution in (4) gives as a first approximation the function $h_0(T)$ shown in Fig. 8. $h_0(T)$ contains a sharp and physically implausible negative cusp which reflects the cusp at T_C in $F(T)$. Elimination of the objectionable cusp requires modification of $F(T)$ to moderate the extremely rapid rise that occurs close to T_C.

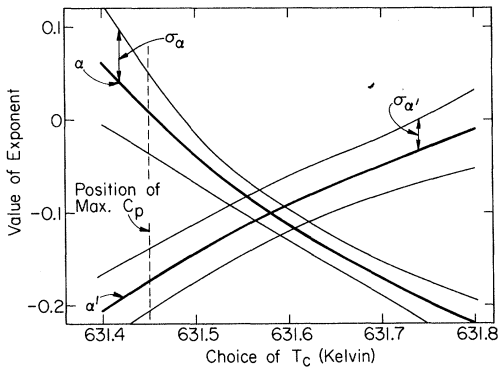

FIG. 7. Variation of exponents α and α' as a function of T_C. Light curves indicate variation of the estimated statistical uncertainty σ_α.

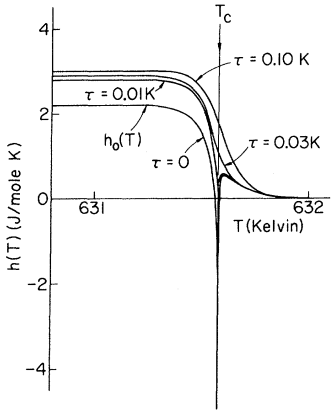

FIG. 8. Interpolation function $h(T)$ obtained from (4). The effect of substituting (5) for t in $F(T)$ is shown for several values of τ.

An analytic expression which accomplishes this has been given by Teany, van der Hoeven, and Moruzzi.[19] The ordinary reduced temperature t is replaced by a "complex" temperature u defined as

$$u \equiv [t^2 + (\tau/T_C)^2]^{1/2} , \tag{5}$$

where τ is a characteristic temperature increment whose value may be chosen to give the best fit to the experimental data. Substitution of u for t in (3a) and (3b) causes the argument of $F(T)$ to approach the constant value τ/T_C as $t \to 0$. In effect, choice of τ permits a rounding of the cusp in $F(T)$ for values of $t < \tau/T_C$, thus providing a better fit to the experimentally observed rounding at T_C.

Since $u \to t$ for $t > \tau/T_C$, substitution of u for t in (3) has negligible effect on the α's, A's, and K's which are determined by the form of the experimental curves away from T_C. However, the substitution does affect the size of Δ which now becomes a function of τ. If, as previously inferred, $\alpha = \alpha'$, then

$$\lim_{T \to T_C} u^{-\alpha} = \lim_{T \to T_C} u^{-\alpha'} = (\tau/T_C)^{-\alpha} \tag{6}$$

and, from (3),

$$\Delta(\tau) = \frac{(A' - A)(\tau/T_C)^{-\alpha}}{\alpha} + (K' - K) . \tag{7}$$

Since $A > A'$, the size of the discontinuity, $\Delta(\tau)$, increases with increasing values of τ. The effect of the choice of τ in modifying the behavior of $h(T)$ is illustrated in Fig. 8. A reasonable looking $h(T)$, free of cusps and ripples, is obtained for the choice $\tau \simeq 0.030$ K.

Recently, McCoy and Wu[20] have pointed out that the rounded transition given by (5) approximates the result obtained in their theoretical analysis of the effect of impurity content on the ferromagnetic transition. Further experimental data on the effect of physical and chemical impurity on the shape of the transition will be presented in Sec. III A 4.

Various authors[21–23] have approached this problem by treating the rounding exhibited by real specimens as the integrated result of a continuous distribution of Curie points centered about an average value T_C. Such a distribution may be regarded as arising from small differences in the critical temperatures of microscopic regions within the specimen. Assuming this distribution to be Gaussian, we use the function

$$f(x) = (1/\lambda\sqrt{2\pi})\, e^{-(x - T_C)^2/2\lambda^2} , \tag{8}$$

where λ is a measure of the half-width of the distribution. The experimental specific heat $C_v^*(T)$ is given by the convolution integral of (1) with (8), i.e.,

$$C_v^*(T) = \int_0^\infty C[t(x)] f(x)\, dx , \tag{9}$$

where $C[t(x)]$ is (1) evaluated for the argument $t(x) = (T - x)/T_C$. Evaluation of (9) was done numerically using the values of T_C, the α's, A's, and K's given in Sec. III A 2, and choosing $\lambda = 0.10\,^\circ$C by trial. The resulting curve, shown by the dashed line in Fig. 5, gives a satisfactory representation of the experimental data throughout the transition region.

The distribution function (8) may also be used to calculate the interpolation function $h(T)$. Applying the definition of (4) to the situation of a continuous distribution of Curie points we have

$$h(T) = C_v^*(T) - F'(T) , \tag{10}$$

where $C_v^*(T)$ is given by (9) and $F'(T)$ is the convolution integral

$$F'(T) = \int_0^\infty F[t(x)] f(x)\, dx \tag{11}$$

and $F[t(x)]$ is the function defined in (3a) and (3b). The resulting $F'(T)$ is qualitatively similar to the result obtained by substituting u for t in (4). Substituting from (9) and (11) in (10) we obtain

$$h(T) = \int_0^\infty \{C[t(x)] - F[t(x)]\} f(x)\, dx$$

$$= \Delta \int_T^\infty f(x)\, dx \tag{12}$$

where, as before, $\Delta = K' - K$. The resulting $h(T)$ is qualitatively similar to the curves shown in Fig. 8 but without the variability in Δ. In fact, it has the same asymtotic form as $h_0(T)$ but is smooth throughout the transition region.

In principle, it should be possible to infer the form of the distribution function $f(x)$ from the experimentally measured $C_v^*(T)$ by solving (9). However, the present data are described to within the accuracy of measurement by the assumed Gaussian distribution (7). No clear theoretical basis for deriving $f(x)$ appears to exist at present. Further

work is required to identify the physical variables responsible for the rounding of the specific-heat maximum. Some preliminary observations are described in Sec. III A 4.

4. *Physical Influence on Rounding*

It is well known that alloying additions to Ni change the apparent T_C and also cause significant rounding.[9,24] McCoy and Wu[20] have pointed out that, at low concentration levels, physical impurity (i.e., vacancies, dislocations, or isotopic mixtures) should produce effects comparable to that resulting from chemical impurity.

Mass-spectroscopic analysis was made of the signal-crystalline Ni specimen after the specific-heat measurements. The principal impurities present were (in ppm at.%) Cu(58), Co(793), Fe(114) Si(990), Al(140), and Na(256). (This represents a substantial degradation from the purity of the starting material from which the single crystal was prepared. Efforts are continuing to produce cleaner single crystals.) The relatively large impurity content seemed a likely cause of the observed rounding.

To check this surmise, specific-heat measurements were made on an analytically verified specimen of 99.999% Ni polycrystalline foil of 0.025 mm thickness. The results are shown as curve B in Fig. 9 where curve A shows the single-crystal data for comparison. It is evident that the impure crystal has an appreciably sharper transition. Apparently, the polycrystalline structure (grain size ~ 0.03–0.10 mm) is more important than the chemical impurity.

To pursue the effect of crystalline imperfection, a specimen of the same impure single-crystalline Ni was deformed (by mashing between hardened and polished steel plates in a press) to 60% of its original thickness. The specific heat was then measured in the deformed state (without the usual annealing treatment). The resulting curve, shown as C in Fig. 9, shows the greatest degree of rounding observed.

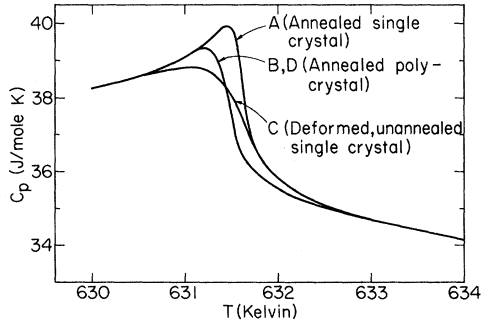

FIG. 9. Effects of crystalline imperfection on the apparent rounding of the specific-heat maximum at T_C.

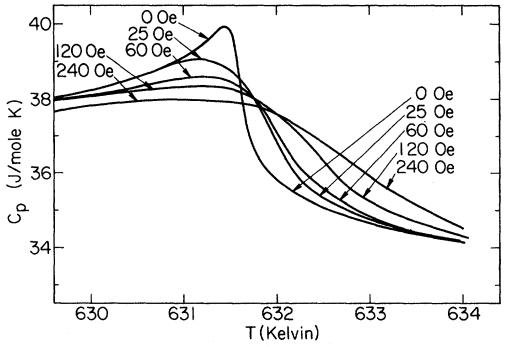

FIG. 10. C_p for single-crystal Ni in various magnetic fields applied parallel to the plane of the specimen.

Finally, the deformed specimen was subjected to the standard annealing treatment (750 °C for about 5 h), during which recrystallization occured yielding a grain size ~ 0.1–0.3 mm. Upon remeasurement of the specific heat, it was found that the results (curve D of Fig. 9) were indistinguishable from the data obtained with the high-purity polycrystalline foil.

These results indicate that the dislocation density (which was greatest in curve C) has a much greater effect on the rounding than the approximately 0.1% impurity present in the annealed single crystal. Further study of the effect of physical and chemical impurity is in progress.

B. Effect of Applied Magnetic Field

Preliminary measurements have been made of the effect on $C_v^*(T)$ of magnetic fields up to 240 Oe. The field was applied parallel to the plane of the specimen (i.e., the direction of minimum demagnetizing factor). With the present experimental resolution, a parallel field of about 4 Oe is the minimum field for which a detectable change in $C_p(T)$ can be seen. These results are plotted for the temperature range near T_C in Fig. 10. For all field values, the $C_v^*(H, T)$ curves join smoothly although the temperature interval of observable displacement in C_v^* increases with increasing field.

With increasing field, the pattern of displacement in the $C_v^*(H, T)$ curves is that expected from the thermodynamic relation

$$\left(\frac{\partial C_H}{\partial H}\right)_T = T\left(\frac{\partial^2 M}{\partial T^2}\right)_H ,$$

where C_H denotes the specific heat at constant field and M is the specimen magnetization. In other words, the field-induced displacement of the spe-

cific heat is proportional to the curvature of $M(T)$.[25]

Griffiths[26] has proposed that the specific-heat data should scale according to the relation

$$(C_h - C_0)h^{\alpha/\beta\delta} = g(t/h^{1/\beta\delta}) , \qquad (13)$$

where g is an undetermined function of the parameter $t/h^{1/\beta\delta}$. The exponential constants β and δ, respectively, specify the power-law dependence of the magnetization on the reduced temperature t and reduced field h. α is the same constant introduced in (1). Griffiths's relation is inferred from the assumption of a unique magnetic equation of state whose existence has been experimentally confirmed.[27] The experimental variables $C_v^*(H, T)$ and H are normalized by defining a reduced field $h \equiv HM_0/kT_C$ and letting $C_h \equiv C_v^*(H, T)/R$, where M_0 is the saturation magnetization at $T = 0$ K ($M_0 = 0.616$ μ_B/atom[28]), k is Boltzmann's constant, and R is the universal gas constant.

The constant $\beta = 0.378$ is obtained from magnetization data[27] and the present $C_v^*(T)$ data give $\alpha = -0.10$. Applying the scaling law[18]

$$2 - \alpha = \beta(\delta + 1) ,$$

with these values of α and β, gives $\delta = 4.6$, a value which is also consistent with the magnetization data.[27]

Figure 11 is a test of (13) with data for all field values plotted as $(C_n - C_0)\, h^{\alpha/\beta\delta}$ vs $t/h^{1/\beta\delta}$. When scaled in this way, the $C_v^*(H, T)$ values coincide very well below T_C and fairly well above T_C. Data for magnetic fields about 100 times greater than used here have been reported recently by Korn and Kohlhaas.[29] When plotted in the form of Fig. 11, their data show substantial scatter although the qualitative shape is the same as for our low-field results. We believe the increased scatter shown by the Korn and Kohlhaas results is probably related to their difficulty in obtaining precise values of $C_v^*(T)$ in zero field.

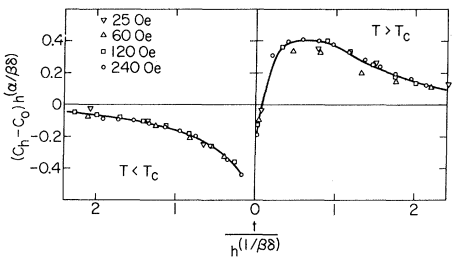

FIG. 11. Scaled plot of specific heat of Ni for several values of applied magnetic field.

IV. DISCUSSION

The present finding that $\alpha = \alpha' = -0.10$ is consistent with current theoretical understanding, agreeing exactly (although perhaps fortuitously) with the theoretical calculation of Jasnow and Wortis[30] which is based on the classical Heisenberg model. It also shows excellent consistency with magnetization data which are related via the scaling law

$$2 - \alpha = \beta(\delta + 1) .$$

Kouvel and Comly[27] have reported the values $\beta = 0.37 \pm 0.004$ and $\delta = 4.58 \pm 0.05$, from which we have

$$\beta(\delta + 1) = 2.11 \pm 0.04 .$$

This is to be compared with our value

$$2 - \alpha = 2.10 \pm 0.03 .$$

As noted in Sec. III our preliminary measurements of the effect of a magnetic field on the specific heat provide further support to the scaling law relating α, β, and δ. Since the field dependence of the specific heat is directly related to the magnetic equation of state, it should be possible to calculate $C_v^*(H, T)$ from magnetization data. However, the analytic expressions for the magnetic equation of state used thus far do not readily yield the experimental values of $C_v^*(T)$ for $H = 0$.

The criterion used to determine T_C in the present work (for $H = 0$) indicates the value to lie close to the temperature at which $(\partial^2 M/\partial T^2)_H = 0$. Our measurements in applied fields (see Fig. 10) indicate this point to be relatively insensitive to the magnitude of the field. Similar conclusions apply to the data of Korn and Kohlhaus for much larger fields. In both cases, the amount of shift in the inflection point of the M-vs-T curves is within the experimental error in T over the observed range of applied field. If it is valid to generalize from the observations at $H = 0$ and define T_C as the temperature of the inflection point in the magnetization curves at constant field, then it follows that T_C is not appreciably shifted by an applied field.

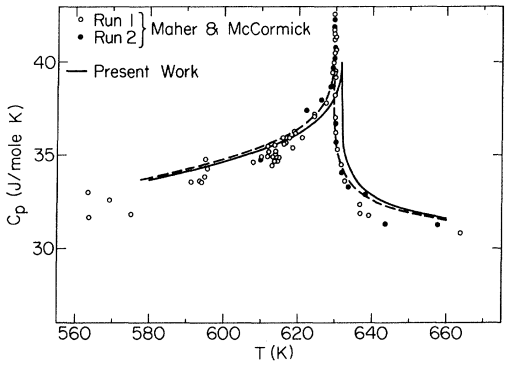

FIG. 12. Comparison of present data with values reported in Ref. 17. Solid curve gives values of Table I. Agreement is improved by reducing our T values by about 2 K as shown by dashed curve.

A substantial field-dependent shift in T_C of Ni has been reported recently by Drabkin *et al.*[31] on the basis of scattering experiments using polarized thermal neutrons. The value reported is $\Delta T_C \sim -1.0$ K at $H = 20$ Oe and it varies as H^2 for smaller fields. Referring to the curve for $H = 25$ Oe shown in Fig. 10, the value of Drabkin *et al.* is about the same as the half-width of the temperature range (symmetric about T_C) in which C_p is shifted from the $H = 0$ curve. Drabkin *et al.* do not explain how their neutron intensity data can be related to T_C and we believe their interpretation is doubtful. The evidence of Fig. 10 suggests that their neutron data indicate the onset of the field-induced rounding of the transition and are not characteristic of T_C.

Our experimental results show important differences when compared with the recently reported work of Maher and McCormick (MM).[17] In terms of basic observables, the nature of the difference can be presented graphically by plotting C_p vs T for the two investigations as is done in Figs. 12 and 13. The data of MM are shown by the discrete points while the continuous indication of the present measurements is shown by the strip whose width represents our estimated experimental uncertainty.

Over the 100-K span covered by both investigations there is reasonably good agreement, although the experimental scatter of the MM data is noticeably larger than ours. Agreement is slightly improved by shifting our temperature scale downward by about 2 K to make the observed position of our maximum in C_p coincide with the MM result.[32]

Within ± 0.1 K of the Curie point, a tight cluster of data points appear to define a sharp cusp with a maximum value about 5% greater than indicated by our ac measurements. These data are interpreted by MM to indicate a power-law dependence of the form of (1) which holds for $t \geq 10^{-5}$. The same data are plotted with a greatly expanded T scale in Fig. 13. It will be noted that our data, recorded continuously and with an experimental resolution at least equal to that claimed by MM, fail to show any indication of the sharp cusp at T_C. Thus the two measurements disagree on a basic qualitative feature of the transition.

The source of this disagreement must presumably be explained in terms of the differing procedures followed in the two measurements. The MM data were obtained on one 17-g specimen of single-crystalline Ni whereas the present data were found reproducible for 6 different (but much smaller) single-crystalline specimens. On the basis of information provided by the supplier of MM's specimen it was probably purer than ours but no confirming analysis is available. However, the observations described in Sec. III A 4 indicate the contribution of chemical purity to rounding to be less important than physical imperfection. The MM data were obtained following the conventional procedures of adiabatic calorimetry but, by careful technical refinements, using temperature rises of the order of 0.01 K to obtain the desired resolution. Rather than attempting an absolute determination of C_p, their experimental values were normalized to fit an average of previously published C_p data in substantially the manner used in treating our own data.

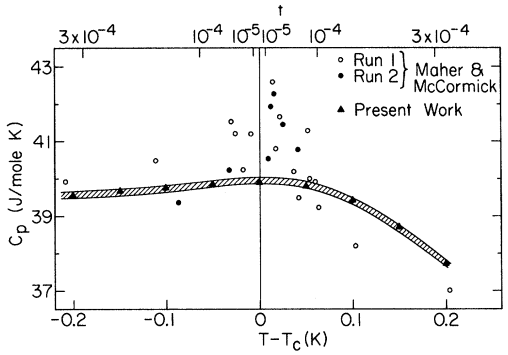

FIG. 13. Comparison of present data with values of Ref. 17 in a temperature range very close to the specific-heat maximum. The shaded band represents the estimated relative experimental uncertainty in our C_p values.

Considering all the known differences in the two measurements, the reason for the discrepancy in the apparent sharpness of the transition remains obscure. Further efforts are now in progress to see whether sharper transitions in Ni can be obtained using the ac method.

ACKNOWLEDGMENTS

We are obliged to many colleagues for their interest and comments on this work but we wish to express our special appreciation to the following: Our attention was originally directed to this problem by L. P. Kadanoff, who has given both encouragement and advice. H. K. Birnbaum provided the single-crystal Ni specimen and gave valuable assistance on all our metallurgical problems. M. Rayl was an enthusiastic collaborator in the early phases of this work. The mass-spectrographic analyses of various Ni specimens were done by V. G. Mossotti and W. C. Phillips. Many difficult technical problems in the fabrication of the apparatus were surmounted through the skillful assistance of W. L. Craig and N. Vassos.

*Work supported in part by the Advanced Research Projects Agency under Contract No. HC 15-67-C-0221, and in part by the U. S. Army Research Office (Durham).

[1]Y. A. Kraftmakher, Zh. Prikl. Mekhan. i Tekhn. Fiz. 5, 176 (1962).

[2]Paul F. Sullivan and G. Seidel, Phys. Rev. 173, 679 (1968).

[3]Paul Handler, D. E. Mapother, and M. Rayl, Phys.

Rev. Letters 19, 356 (1967).

[4]Very stable light intensity at constant current was obtained with a GE Quartzline iodide cycle bulb specified as No. 6.6A/T2-1/2Q/CL-452 and available from GE Lamp Division, Nela Park, Cleveland, Ohio.

[5]Model No. RDE-1 radiation thermocouple, Charles Reeder and Co., Detroit, Mich.

[6]Type No. 2111A frequency standard, American Time Products, Inc., New York, N.Y.

[7]Material supplied by the High-Purity Metals Division, United Mineral and Chemical Co., New York, N. Y.

[8]Electro-glo Co., Chicago, Ill.

[9]R. E. Pawel and E. E. Stansbury, J. Phys. Chem. Solids 26, 607 (1965).

[10]M. Braun and R. Kohlhaas, Phys. Status Solidi 12, 429 (1965).

[11]C. Sykes and H. Wilkinson, Proc. Phys. Soc. (London) 50, 834 (1938).

[12]R. E. Pawel and E. E. Stansbury, J. Phys. Chem. Solids 26, 757 (1965).

[13]A. B. Pippard, *Elements of Classical Thermodynamics* (Cambridge U. P., Cambridge, England, 1957), p. 143.

[14]L. Patrick, Phys. Rev. 93, 384 (1954).

[15]F. C. Nix and D. McNair, Phys. Rev. 60, 597 (1941).

[16]Hereafter, the unsubscripted symbol $C(t)$ is used to denote the analytic function defined in (1), to differentiate it from the experimentally derived magnetic specific heat C_v^*. It is desirable to observe this distinction since it will be shown that a satisfactory fit to C_v^* near T_C cannot be obtained by adjusting the constants in (1).

[17]Warren E. Maher and William D. McCormick, Phys. Rev. 183, 573 (1969).

[18]L. P. Kadanoff *et al.*, Rev. Mod. Phys. 39, 395 (1967).

[19]Dale T. Teany, B. J. C. van der Hoeven, Jr., and V. L. Moruzzi, Phys. Rev. Letters 20, 722 (1968).

[20]Barry M. McCoy and Tai Tsun Wu, Phys. Rev. Letters 21, 549 (1968).

[21]T. Yamamoto, O. Tanimoto, Y. Yasuda, and K. Okada, in *Critical Phenomena, Proceedings of a Conference, Washington, D. C.*, 1965, edited by M. S. Green and J. V. Sengers, Natl. Bur. Std., Miscellaneous Publication No. 273 (U.S. GPO, Washington, D. C., 1966), pp. 86–91.

[22]J. Skalyo, Jr. and S. A. Friedberg, Phys. Rev. Letters 13, 33 (1964).

[23]R. B. Griffiths (private communication).

[24]R. M. Bozorth, *Ferromagnetism* (Van Nostrand, New York, 1951).

[25]Extensive data on M(H, T) for Ni have been given by P. Weiss and R. Forrer, Ann. Phys. (Paris) 5, 153 (1926).

[26]R. B. Griffiths, Phys. Rev. 188, 942 (1969); also private communication.

[27]J. S. Kouvel and J. B. Comly, Phys. Rev. Letters 20, 1237 (1968).

[28]H. Danan, A. Herr, and A. J. P. Meyer, J. Appl. Phys. 39, 669 (1968).

[29]J. Korn and R. Kohlhaas, Z. Angew. Phys. 26, 119 (1969).

[30]David Jasnow and Michael Wortis, Phys. Rev. 176, 739 (1968).

[31]G. M. Drabkin, A. I. Okorokov, E. I. Zabidarov, and Ya. A. Kasman, Zh. Eksperim. i Teor. Fiz. Pis'ma v Redaktsiyu 8, 549 (1968) [Soviet Phys. JETP Letters 8, 335 (1968)].

[32]The need for such a shift indicates a discrepancy between the temperature scales used in the two investigations. This is mildly surprising since we both used the same model of commercially available calibrated platinum resistance thermometer for standardization. Although the absolute value of T_c is of secondary importance in these measurements, this discrepancy illustrates the considerable experimental difficulty of obtaining reliable absolute temperature values in this range.

PHYSICAL REVIEW B VOLUME 3, NUMBER 3 1 FEBRUARY 1971

Heat Capacities of $Fe(HCOO)_2 \cdot 2H_2O$ and $Ni(HCOO)_2 \cdot 2H_2O$ between 1.4 and 20 °K†

R. D. Pierce* and S. A. Friedberg
Carnegie-Mellon University, Pittsburgh, Pennsylvania 15213
(Received 24 August 1970)

The heat capacities of $Fe(HCOO)_2 \cdot 2H_2O$ and $Ni(HCOO)_2 \cdot 2H_2O$ have been measured between 1.4 and 20 °K. Peaks associated with long-range spin ordering are found at 3.74 °K for $Fe(HCOO)_2 \cdot 2H_2O$ and at 14.5 °K for $Ni(HCOO)_2 \cdot 2H_2O$. An additional Schottky-like maximum occurs at 3 °K in the heat capacity of the nickel salt. These anomalies can be correlated with corresponding features of the observed magnetic susceptibilities. A unit cell of these salts contains two each of two inequivalent metal ions, types *A* and *B*. Formate groups form *AA* and *AB* bridges and are thought to mediate the dominant superexchange interactions. The thermal data show that the *AB* interaction is much weaker than the *AA* interaction in $Ni(HCOO)_2 \cdot 2H_2O$; for $Fe(HCOO)_2 \cdot 2H_2O$ their relative strengths could not be determined.

INTRODUCTION

In a previous paper[1] we described measurements of the low-temperature heat capacity of manganous formate dihydrate, $Mn(HCOO)_2 \cdot 2H_2O$. In this paper we report the heat capacities of the related salts $Fe(HCOO)_2 \cdot 2H_2O$ and $Ni(HCOO)_2 \cdot 2H_2O$.

Ferrous formate dihydrate[2] and nickelous formate dihydrate[3] have both been shown to be isostructural with $Mn(HCOO)_2 \cdot 2H_2O$.[4] The structure of